A Decentralized Stay-Time Based Occupant Distribution Estimation Method for Buildings

Qing-Shan Jia, *Senior Member, IEEE*, Hengtao Wang, *Member, IEEE*, Yulin Lei, *Member, IEEE*, Qianchuan Zhao, *Senior Member, IEEE*, and Xiaohong Guan, *Fellow, IEEE*

***Abstract*—Zonal occupant level is of great practical interest for building energy saving under normal operations and for fast evacuation under emergency. Though there are many existing sensing systems to estimate this information, the problem is still challenging due to the privacy concerns, the random human movement, and the accumulative error. In this paper, we consider this important problem and focus on infrared beam systems that monitor the zonal arrival and departure events. We make the following contributions. First, a rule (i.e., Rule 1) based on the stay time is developed to reduce the accumulated estimation error in each zone. Second, a rule (i.e., Rule 2) is designed to coordinate the estimation among neighboring zones. A decentralized estimation method is then developed using these two rules. Third, the advantage of this method is demonstrated through simulation results and field tests. We hope this work brings insight to zonal occupant level estimation in buildings in more general situations.**

***Note to Practitioners*— This paper is motivated by the zonal occupant-level estimation problem in buildings. Infrared beam sensors are considered in this paper due to the privacy concern and the low cost. An estimation method is developed to use the stay time of the occupants to correct the local estimation and to propagate the corrections among neighboring zones to keep the total number of occupants as a constant. Both simulation results and field tests are used to demonstrate the performance of this method. This method can be easily implemented in a decentralized way, which is a salient feature especially for large-scale commercial buildings.**

***Index Terms*—Building energy saving, discrete event dynamic system, occupant level estimation, wireless sensor network.**

Manuscript received December 16, 2013; revised July 04, 2014; accepted September 21, 2014. Date of publication October 21, 2014; date of current version October 02, 2015. This paper was recommended for publication by Associate Editor Q. Huang and Editor L. Shi. This work was supported in part by the Tsinghua-UTC Research Institute for Building Energy, Safety and Control Systems, the United Technologies Research Center, the National Natural Science Foundation of China under Grants 60704008, 60736027, 61021063, 61074034, 61174072, 61222302, 90924001, 91224008, and U1301254, the 111 International Collaboration Program of China under Grant B06002, TNList Funding for Cross Disciplinary Research, and the Specialized Research Fund for the Doctoral Program of Higher Education under Grant 20070003110. *(Corresponding author: Qing-Shan Jia.)*

Q.-S. Jia, H. Wang, Y. Lei, and Q. Zhao are with the Center for Intelligent and Networked Systems (CFINS), Department of Automation, TNList, FIT-3-611, Tsinghua University, Beijing 100084, China (e-mail: jiaqs@tsinghua.edu.cn; wanght07@mails.tsinghua.edu.cn; leiyl11@mails.tsinghua.edu.cn; zhaoqc@tsinghua.edu.cn).

X. Guan is with the Center for Intelligent and Networked Systems (CFINS), Department of Automation, TNList, FIT-3-616, Tsinghua University, Beijing 100084, China, and also with the MOE KLINNS Lab, Xi'an Jiaotong University, Xi'an 710049, China (e-mail: xhguan@tsinghua.edu.cn).

This paper has supplementary downloadable multimedia material available at http://ieeexplore.ieee.org provided by the authors. The Supplementary Material includes slides in PDF format. This material is 982 MB in size.

Color versions of one or more of the figures in this paper are available online at http://ieeexplore.ieee.org.

Digital Object Identifier 10.1109/TASE.2014.2361122

I. Introduction

BUILDING is responsible for more than 30% of the energy consumed in developed and developing countries [1] and has great energy saving potential. The advances in sensing and control technology now provide the opportunity to improve the energy efficiency, comfort, and safety in buildings bsimultaneously. Occupant distribution is an important information to achieve this goal. Commercial office buildings are composed of multiple zones [2], [3]. A zone could be a room, a corridor, or a sector of a floor. Zonal occupant level is the number of occupants in a zone. This information can be used to predict the heating and cooling load of each zone and therefore to coordinate the heating, ventilation, and air conditioning (HVAC) system and energy-storage devices to improve the energy efficiency of the building under normal conditions [4], [5]. Under emergent conditions, this information can not only provide an initial condition to generate an evacuation plan, but also adjust the guidance in real time to avoid congestion [6]. Therefore, zonal occupant-level estimation is of great practical interest.

Many systems can be used to estimate zonal occupant level, which can be classified into two groups. The first group requires collaboration from the occupants. Usually, the occupant is required to wear a tag. Then, the problem is converted to locate and to track the tag. These systems usually suffer from privacy concerns. Also when the occupants are detached from the tags either accidentally or intentionally, the estimated occupant level is subject to large estimation error. On the contrary, the second group does not require such a collaboration. Infrared, video, CO_2 sensors are such examples. These systems (except for the video systems) do not reveal the identity of the occupant and therefore protect the privacy. The sensors are usually installed in fixed positions and powered by wired power lines. Due to these advantages, sensing systems in this group has received more and more attention recently. More detailed review on the various sensing systems will be provided in Section II.

Despite the aforementioned existing systems, the occupant-level estimation is still nontrivial in general due to the privacy concern, the random human movement, and the balance between the estimation accuracy and the cost. In this paper, we consider an infrared beam sensing system. These sensors are deployed at the boarders among the zones. As shown in Fig. 1, each set contains a pair of infrared beam sensors. When an occupant crosses the boarder, the two beams will be blocked in sequence. In this way, we can detect such a boarder crossing event and identify if it is an arrival or a departure event to a zone. This

Fig. 1. Each boarder sensor contains a pair of infrared beam sensors.

system does not reveal the identity of the occupant and has a low cost and a high accuracy to detect the boarder crossing event. A naive estimation method is to use the difference between the number of arrival and departure events to a zone as an estimate of the remaining occupant level. Though this method is well adopted in many commercial systems, it suffers from accumulated error. In other words, when a sensing error occurs (either a false alarm or a misdetection), such an error remains in the estimation until the system is reset.

In this paper, we develop an estimation method to improve the estimation accuracy. This method is based on two observations. The first observation is that when there are a large number of occupants in a zone a departure event usually happens within a short period of time. On the contrary, when there are a small number of occupants in a zone, departure may occur after a long period of time. Based on this observation, we develop a rule to adjust the estimated occupant level according to the stay time of the occupants in a zone. This is denoted as rule 1. The second observation is the conservation of occupants. In other words, when occupants travel among the zones, the total number of occupants in these zones should keep constant. Thus, when an estimation error is identified by rule 1 and a correction term is generated to improve the estimation accuracy of the current zone, such a correction term is also used to correct some neighboring zones, according to the transition probability of the occupant from (or to) the neighboring zones. This is denoted as rule 2. More details of these rules will be shown in Section IV. Based on these two rules, a decentralized estimation method is then developed and demonstrated by simulation and field tests.

The remainder of this paper is organized as follows. We briefly review related literature in Section II, mathematically formulate the occupant level estimation problem in Section III, provide the two rules, and the estimation method in Section IV, demonstrate the performance of the method using simulation and field tests in Section V, and conclude in Section VI.

II. Literature Review

We briefly review related works in this section. Many sensing systems exist to estimate the zonal occupant level in a building. As aforementioned, these systems can be classified into two groups, namely the one that requires the collaboration from the occupants and the other one that does not. Examples of the first group include RADAR [7], SpotON [8], LANDMARC [9], Ekahau [10], UWB [11], (active and passive) RFIDs[12], Active Badge [13], and Cricket [14]. These systems require the occupants to wear a tag (also called badge or mote in some systems), and then locate and track the movement of the tag. For those that use the received signal strength indicator (RSSI) during the localization, the systems usually suffer from the multi-path effect. For those that use the ultrasonic signals, usually a large number of nodes need to be deployed to cover the entire area. When the occupant is detached from the tag (either intentionally or accidentally), the occupant cannot be localized neither tracked.

Examples of the second group include video cameras, CO_2 sensors, energy consumptions, and infrared. Video cameras [15]–[18] are usually sensitive to background lighting, and violate the privacy of the occupants. CO_2 sensors usually drift and energy sensors in general have low accuracies to estimate the occupant level in a zone [19]. There are two types of infrared sensors, namely the motion sensors and the beam sensors. The motion sensors are also called presence sensors and have been widely applied in many commercial and public buildings to detect whether a zone is occupied or not. Such information can then be used for lighting control and HVAC control. However, when there are multiple occupants in the same zone, motion sensors cannot tell the exact number of the occupants. Infrared beam sensors are usually deployed on the boarders among the zones. They can detect the arrival and departure of the occupant from one zone to another. Infrared sensors (especially those that are only sensitive to a short range of the temperature around 37 °C) barely have false alarms. However, when the corridor is wide and multiple occupants cross the beam sensors at the same time, misdetection usually happens.

Fusion information collected by multiple sensors usually achieves higher estimation accuracies [15], [20], [21]. Various models on human movement under normal and emergent conditions exist [22]–[25]. The occupant-level estimation can be improved using movement models, which will later on be demonstrated by numerical results in this paper.

III. Problem Formulation

Building is composed of multiple zones. A zone could be a room, a corridor, or an aggregation of multiple rooms. Let each zone be a node, and the connections among the zones be the edges. Then the zonal structure of a building can be modeled as a graph. Consider such a graph $G = \{\mathcal{V}, \mathcal{E}\}$, where $\mathcal{V}$ is the set of zones and $\mathcal{E}$ is the set of edges. An edge between zone i and j is denoted as (i, j). Let $N = |\mathcal{V}|$ and $M = |\mathcal{E}|$. For example, the layout of a section of a building is shown in Fig. 2(a). The corresponding graph model is shown in Fig. 2(b).

Consider a discrete time version of the problem, where each stage represents a period of time with length Δ. Then, the kth stage represent the period of time $[k\Delta, (k+1)\Delta)$. To simplify the notation, we will use time k and $k\Delta$ interchangeably in the

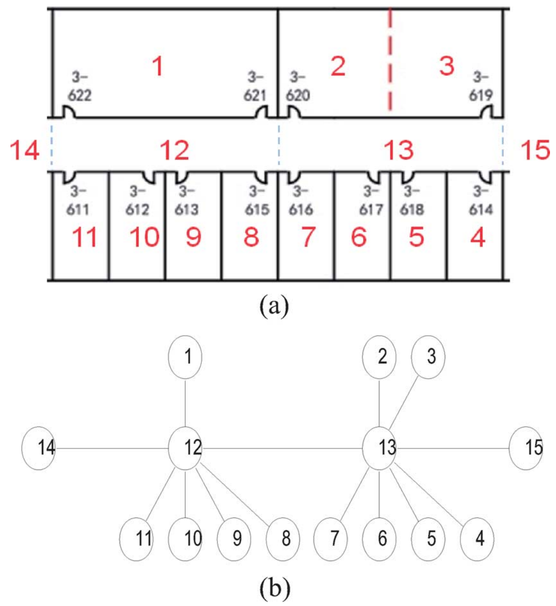

Fig. 2. Layout of a section of a building and the graph model (layout 1).

following. Let $n_i(k)$ be the number of occupants in zone i at time k. Then, $\mathbf{n}(k) = (n_1(k), \ldots, n_N(k))$ is the state vector at k. Let $e_{i,j}(k) \geq 0$ be the number of arrivals from zone i to zone j within the kth stage. Then $\mathbf{e}(k) = (e_{i,j}(k), (i,j) \in \mathcal{E})$ represent the number of arrivals and departures among all of the zones during the kth stage. In stage k, let the total number of arrivals to zone i be $e_{*,i}(k)$ and the total number of departures from zone i be $e_{i,*}(k)$, i.e.,

$$e_{*,i}(k) = \sum_{j \in \mathcal{V}, (j,i) \in \mathcal{E}} e_{j,i}(k)$$
$$e_{i,*}(k) = \sum_{j \in \mathcal{V}, (i,j) \in \mathcal{E}} e_{i,j}(k).$$

A. Sensor Model

There are infrared beam sensors deployed at all of the boarders among the zones that can detect the boarder-crossing events. Let $\hat{e}_{i,j}(k)$ denote the observed number of movements from zone i to j in stage k. Due to the sensing error, we usually have $\hat{e}_{i,j}(k) \neq e_{i,j}(k)$. In particular, when there is a single arrival from zone i to j in k, i.e., $e_{i,j}(k) = 1$, we assume that

$$\begin{aligned}
\Pr\{\hat{e}_{i,j}(k) = -1 | e_{i,j}(k) = 1\} &= p_s^{-1} \\
\Pr\{\hat{e}_{i,j}(k) = 0 | e_{i,j}(k) = 1\} &= p_s^{0} \\
\Pr\{\hat{e}_{i,j}(k) = 1 | e_{i,j}(k) = 1\} &= p_s^{1} \\
\Pr\{|\hat{e}_{i,j}(k)| > 1 | e_{i,j}(k) = 1\} &= 0
\end{aligned}$$

where $p_s^{-1}, p_s^0, p_s^1 \geq 0$ and $p_s^{-1} + p_s^0 + p_s^1 = 1$. Similarly, we can define

$$\hat{e}_{*,i}(k) = \sum_{j \in \mathcal{V}, (j,i) \in \mathcal{E}} \hat{e}_{j,i}(k),$$
$$\hat{e}_{i,*}(k) = \sum_{j \in \mathcal{V}, (i,j) \in \mathcal{E}} \hat{e}_{i,j}(k).$$

Let $\hat{\mathbf{e}}(k) = (\hat{e}_{i,j}(k), (i,j) \in \mathcal{E})$. Assume the sensing error for all the arrivals (and departures) are independent. When there are multiple arrivals from zone i to j in k, i.e., $e_{i,j}(k) = e > 1$, we have

$$\begin{aligned}
&\Pr\{\hat{e}_{i,j}(k) = \hat{e} | e_{i,j}(k) = e\} \\
&\quad = \sum_{\hat{e}_1 + \cdots \hat{e}_e = \hat{e}} \prod_{\tau=1}^{e} \Pr\{\hat{e}_{i,j}(k) = \hat{e}_\tau | e_{i,j}(k) = 1\}.
\end{aligned}$$

Infrared beam sensors usually do not have false alarms. Thus, we have

$$\Pr\{\hat{e}_{i,j}(k) > 0 | e_{i,j}(k) = 0\} = 0.$$

B. Occupant Movement Model

We use a Markov chain to approximate the movement of the occupants. Let $p_{i,j}$ denote the probability for an occupant to move from zone i to zone j within a stage. Then, we have

$$\sum_{j \in \mathcal{V}} p_{i,j} = 1.$$

Assume that the movement of the occupants is identically independent.

C. Estimation Problem

Note that we have

$$n_i(k+1) = n_i(k) - e_{i,*}(k) + e_{*,i}(k)$$

which shows that the total number of occupants in zone i at $k + 1$ equals the occupant level in this zone at k adjusted by the total number of arrivals and departures during the kth stage. Let $\bar{n}_i(k)$ be the estimated number of occupants in zone i at k, and $\hat{n}_i(k+1)$ be the observed number of occupants in zone i at $k + 1$. Then, we have

$$\hat{n}_i(k+1) = \bar{n}_i(k) - \hat{e}_{i,*}(k) + \hat{e}_{*,i}(k).$$

A naive estimation (NE) algorithm uses $\hat{n}_i(k+1)$ as an estimate of $n_i(k+1)$, i.e., $\bar{n}_i^{\mathrm{NE}}(k+1) = \hat{n}_i^{\mathrm{NE}}(k+1)$. However, this estimation may be poor due to the accumulation of the sensing error. Instead, a correction term $n_i^{\Delta}(k+1)$ is used to improve the estimation, i.e.,

$$\bar{n}_i(k+1) = \hat{n}_i(k+1) + n_i^{\Delta}(k+1). \tag{1}$$

There are different performance metrics for an estimation. We use error rate in this paper. The error rate at time k is defined as

$$c(\mathbf{n}(k), \bar{\mathbf{n}}(k)) = \frac{\sum_{i=1}^{M} |n_i(k) - \bar{n}_i(k)|}{2Z} \tag{2}$$

where Z is the total number of occupants in the zones. Note that under the conservation of the total number of occupants, each single miss-count/over-count causes error in two zones. Therefore the error rate in (2) is adjusted by a factor of 2 in the

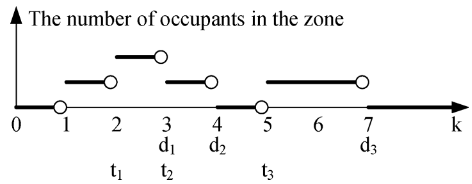

Fig. 3. Sample path of the occupant level in zone i.

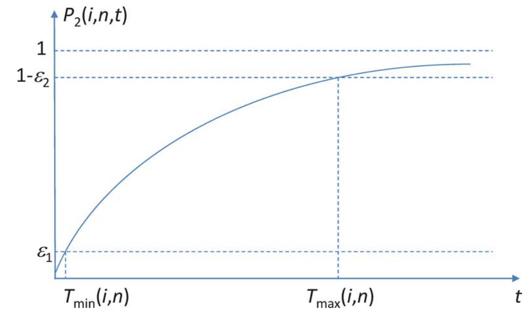

Fig. 4. Relationship among ϵ_1, ϵ_2, $T_{\min}$, and $T_{\max}$.

denominator. We are interested in the average error rate over the given T stages, i.e.,

$$f(L) = \frac{1}{T}\mathbf{E}\left[\sum_{k=1}^{T} c(\mathbf{n}(k), L(\mathcal{H}(k-1)))\right] \tag{3}$$

where $\mathcal{H}(k-1) = (\Pi_0, \hat{\mathbf{e}}(1), \ldots, \hat{\mathbf{e}}(k-1))$ represents all of the historical information that is available at time k including the *a priori* knowledge of the initial occupant distribution Π_0, and the observed events in each of the stage $1, \ldots, k-1$. Policy L is a mapping from the space of all of history until time k to the space of estimated occupant distribution. We want to find a policy to minimize $f(L)$, i.e.,

$$\min_L f(L). \tag{4}$$

Note that each policy L generates a correction term $n_i^{\Delta}(k+1)$ in (1). In other words, we are interested in a policy that can generate the correction terms to minimize the average error rate.

IV. Main Results

A. Two Rules

We have the following two observations. First, people do not stay in a zone forever. When there are a large number of occupants in a zone, a departure usually happens within a short period of time. Second, the total number of occupants in all of the zones does not change when occupants move among the zones. Based on these two observations, we provide two rules.

1) Rule 1—Correction Generation: The idea is to adjust the estimation of the occupant level in a single zone based on the stay time. Consider a sample path of the occupancy level in zone i, $\{n_i(k), k = 1, \ldots, T\}$. Suppose the departure events occur at time $\{d_1, d_2, \ldots\}$ and the last (arrival or departure) event before the jth departure occurs at time t_j. Then, we have a sequence of pairs $\{(n_i(t_j), d_j - t_j), j = 1, 2, \ldots\}$. Each such pair means that there are $n_i(t_j)$ occupants in the zone and one of them leaves after $d_j - t_j$ units of time. We show one example in Fig. 3. Because the occupants follow independent identically Markovian movement model, we have

$$\begin{aligned}
&P_1(i,n,t)\\
&\quad = \Pr\{\text{No departure within } t \text{ stages} | n_i(k) = n\}\\
&\quad = \left(p_{i,i}^t\right)^n.\\
&P_2(i,n,t)\\
&\quad = \Pr\{\text{The next departure is within } t \text{ stages} | n_i(k) = n\}\\
&\quad = 1 - \left(p_{i,i}^t\right)^n.
\end{aligned}$$

Let us define

$$\begin{aligned}
T_{\min}(i,n) &= \max\{t | P_1(i,n,t) \le \epsilon_1\}\\
T_{\max}(i,n) &= \min\{t | P_2(i,n,t) \le \epsilon_2\}
\end{aligned}$$

where $\epsilon_1, \epsilon_2 \in [0,1]$ are two constants that are set by the user. The relationship among ϵ_1, ϵ_2, $T_{\min}$, and $T_{\max}$ are shown in Fig. 4.

By taking small values of ϵ_1 and ϵ_2, this means that, if there are n occupants in zone i, then with a large probability one should expect to see a departure within $[T_{\min}(i,n), T_{\max}(i,n)]$ stages. In other words, if one has an infinite long sample path, and obtains $\{d_j - t_j, j = 1, 2, \ldots\}$, then

$$\begin{aligned}
&\lim_{J\to+\infty} \frac{1}{J}\sum_{j=1}^{J} I\left(d_j - t_j \le T_{\min}\left(i, n_i(t_j)\right)\right) \le \epsilon_1\\
&\lim_{J\to+\infty} \frac{1}{J}\sum_{j=1}^{J} I\left(d_j - t_j > T_{\max}\left(i, n_i(t_j)\right)\right) \le \epsilon_2
\end{aligned}$$

where $I(A)$ is an indicator function, $I(A) = 1$ (or 0) if the event A is true (or false).

In practice, due to the sensing error, we do not know the sample path $\{n_i(k), k = 1, \ldots\}$ for sure. Instead, we have a sample path of the estimated occupancy level $\{\bar{n}_i(k), k = 1, \ldots\}$. Then, we can define the estimated values $\bar{d}_j$ and $\bar{t}_j$, respectively. Then, we define

$$\begin{aligned}
\bar{\sigma}_{\min} &= \frac{1}{J}\sum_{j=1}^{J} I\left(\bar{d}_j - \bar{t}_j \le T_{\min}\left(i, \bar{n}_i(\bar{t}_j)\right)\right)\\
\bar{\sigma}_{\max} &= \frac{1}{J}\sum_{j=1}^{J} I\left(\bar{d}_j - \bar{t}_j > T_{\max}\left(i, \bar{n}_i(\bar{t}_j)\right)\right)
\end{aligned}$$

where J is the total number of departures that have been observed in zone i so far. If $\bar{\sigma}_{\min} > \epsilon_1$, this means that the departures happen faster than expected. This implies that there are more occupants in zone i than estimated. If $\bar{\sigma}_{\max} > \epsilon_2$, this means that the departures happen slower than expected. This implies that there are less occupants in zone i than estimated. Also note that we always require the estimated value $\bar{n}_i(k) \ge 0$. This leads to the following rule:

$$\begin{aligned}
n_i^{\Delta}(k+1) = &\, I\left(\bar{\sigma}_{\min}(k+1) > \epsilon_1\right) - I\left(\bar{\sigma}_{\max}(k+1) > \epsilon_2\right)\\
&+ I(\hat{n}_i(k+1) + I\left(\bar{\sigma}_{\min}(k+1) > \epsilon_1\right)\\
&- I(\bar{\sigma}_{\max}(k+1) > \epsilon_2) < 0)
\end{aligned}$$

where $\bar{\sigma}_{\min}(k+1)$ and $\bar{\sigma}_{\max}(k+1)$ are the values of $\bar{\sigma}_{\min}$ and $\bar{\sigma}_{\max}$ that are calculated using all of the sample path by stage $k + 1$.

The idea of the correction generation is to correct the estimation if the departures occur significantly faster or slower than expected. In order to justify this idea, we introduce

$$\begin{aligned}
&\Delta_i(n,t)\\
&\equiv \Pr\{\text{The next departure is within } t \text{ stages}|n_i(k)=n+1\}\\
&\quad - \Pr\{\text{The next departure is within } t \text{ stages}|n_i(k)=n\}\\
&= P_2(i,n+1,t) - P_2(i,n,t)\\
&= \left(p_{i,i}^t\right)^n \left(1-p_{i,i}^t\right).
\end{aligned}$$

We have

Theorem 1: If

$$\begin{aligned}
&\Pr\{\text{The next departure is within } t \ stages|n_i(k)=n\}\\
&\quad - \Pr\{\text{The next departure is within } t \text{ stages}|n_i(k)=\bar{n}\}\\
&\geq \Delta_i(\bar{n},t)
\end{aligned}$$

then $n > \bar{n}$.

Proof: We prove by contradiction. Suppose $n \leq \bar{n}$. Then, we have

$$\begin{aligned}
&\Pr\{\text{The next departure is within } t \text{ stages}|n_i(k)=n\}\\
&\quad - \Pr\{\text{The next departure is within } t \text{ stages}|n_i(k)=\bar{n}\}\\
&= \left(p_{i,i}^t\right)^{\bar{n}} - \left(p_{i,i}^t\right)^n\\
&= \left(p_{i,i}^t\right)^{\bar{n}} \left(1-\left(p_{i,i}^t\right)^{n-\bar{n}}\right)\\
&< \left(p_{i,i}^t\right)^{\bar{n}} \left(1-p_{i,i}^t\right)\\
&= \Delta_i(\bar{n},t).
\end{aligned}$$

This contradicts the condition in the theorem. So the assumption that $n \leq \bar{n}$ is wrong. We have $n > \bar{n}$. This completes the proof. ■

Theorem 2: If

$$\begin{aligned}
&\Pr\{\text{The next departure is within } t \text{ stages}|n_i(k)=\bar{n}\}\\
&\quad - \Pr\{\text{The next departure is within } t \text{ stages}|n_i(k)=n\}\\
&\geq \Delta_i(\bar{n}-1,t)
\end{aligned}$$

then $n < \bar{n}$.

Proof: We prove by contradiction. Suppose $n \geq \bar{n}$. Then we have

$$\begin{aligned}
&\Pr\{\text{The next departure is within } t \text{ stages}|n_i(k)=\bar{n}\}\\
&\quad - \Pr\{\text{The next departure is within } t \text{ stages}|n_i(k)=n\}\\
&= \left(p_{i,i}^t\right)^n - \left(p_{i,i}^t\right)^{\bar{n}}\\
&= \left(p_{i,i}^t\right)^n \left(1-\left(p_{i,i}^t\right)^{\bar{n}-n}\right)\\
&< \left(p_{i,i}^t\right)^n \left(1-p_{i,i}^t\right)\\
&= \Delta_i(n,t)\\
&< \Delta_i(\bar{n}-1,t).
\end{aligned}$$

This contradicts the condition in the theorem. So the assumption that $n \geq \bar{n}$ is wrong. We have $n < \bar{n}$. This completes the proof. ■

Theorem 1 shows that if the departures happen faster than expected, then there are more occupants than estimated. Theorem 2 shows that if the departures happen slower than expected, then there are less occupants than estimated. This justifies the idea of rule 1.

2) Rule 2 – Correction Propagation: The idea is that occupants only move among the neighboring zones. Therefore, when a correction $n_i^{\Delta}(k+1) = 1(\text{or } -1)$ is generated for zone i at stage $k+1$, this correction should be propagated to the neighboring zones according to the movement model among these zones. In particular, if $n_i^{\Delta}(k+1) = 1$, this means that there are more occupants in zone i than estimated. This "miscounted" occupant may have come from some neighboring zone $j \in A_i$, where $A_i = \{j|(j,i) \in \mathcal{E}\}$. So there are less occupants than estimated in one of the zones in A_i. To be specific, we have

$$n_j^{\Delta}(k+1) = -1 \text{ w.p. } p_{j,i}^{+1} \equiv \frac{p_{j,i}}{\sum\limits_{l\in A_i} p_{l,i}}$$

where w.p. is short for with probability. If $n_i^{\Delta}(k+1) = -1$, this means that there are less occupants in zone i than estimated. This "overcounted" occupant may have moved to some neighboring zone $j \in A_i$. So there are more occupants than estimated in one of the zones in A_i. To be specific, we have

$$n_j^{\Delta}(k+1) = 1 \text{ w.p. } p_{i,j}^{-1} \equiv \frac{p_{i,j}}{\sum\limits_{l\in A_i} p_{i,l}}.$$

Note that the probabilities $p_{j,i}^{+1}$ and $p_{i,j}^{-1}$ can be estimated from

$$p_{j,i}^{+1} = \frac{\sum\limits_{t=0}^{k} \hat{e}_{j,i}(t)}{\sum\limits_{t=0}^{k} \hat{e}_{*,i}(t)} \tag{5}$$

$$p_{i,j}^{-1} = \frac{\sum\limits_{t=0}^{k} \hat{e}_{i,j}(t)}{\sum\limits_{t=0}^{k} \hat{e}_{i,*}(t)}. \tag{6}$$

Note that $\sum_{j\in A_i} p_{j,i}^{+1} = 1$ and $\sum_{j\in A_i} p_{i,j}^{-1} = 1$.

The idea of correction propagation is to correct the estimates in the neighboring zones to keep the total number of occupants as a constant. When the sensors are identical, miscounted and overcounted events on an edge is proportional to the total number of events that has happened on that edge. This explains (5) and (6).

Algorithm Design

In order to demonstrate the performance of rules 1 and 2, we design three algorithms, namely Algorithm 1, 2, and 3. Algorithm 1 is naive estimation and does not use any rule. Algorithm 2 only uses rule 1 to correct the estimation. Algorithm 3 uses both rules. Note that if each zone has a computing node, then all three algorithms can be implemented in a decentralized way, i.e., the computing node in each zone can update the estimated number of occupants in that zone based on the arrivals and departures to that zone, the correction that is generated by rule 1, and the correction that is propagated from the neighboring zones by rule 2. We will demonstrate the performance of this decentralized version by field test in Section V-B.

Algorithm 1 Naive estimation

1: Initialize $\bar{n}_i(0), i = 1, \ldots, N, k = 0$.
2: Observe $\hat{e}_{i,j}(k), (i,j) \in \mathcal{E}$.
3: **for** $i = 1$ to N **do**
  4: $\hat{n}_i(k+1) = \bar{n}_i(k) - \hat{e}_{i,*}(k) + \hat{e}_{*,i}(k)$.
  5: $\bar{n}_i(k+1) = \max\{n_i(k+1), 0\}$.
6: **end for**
7: $k = k + 1$.
8: **if** $k \leq T$ **then**
  9: Go to step 2.
10: **else**
  11: Stop.
12: **end if**

Algorithm 2 Naive estimation with correction

1: Initialize $\bar{n}_i(0), i = 1, \ldots, N, k = 0$. Set ϵ_1 and ϵ_2.
2: Observe $\hat{e}_{i,j}(k), (i,j) \in \mathcal{E}$.
3: **for** $i = 1$ to N **do**
  4: $\hat{n}_i(k+1) = \bar{n}_i(k) - \hat{e}_{i,*}(k) + \hat{e}_{*,i}(k)$.
  5: Update the series of (occupant level, departure time) pair $\left(\bar{n}_i(\bar{t}_j), \bar{d}_j - \bar{t}_j\right), j = 1, \ldots, J$.
  6: $\bar{\sigma}_{\min}(k+1) = (1/J)\sum_{j=1}^{J} I \left(\bar{d}_j - \bar{t}_j \leq T_{\min}\left(i, \bar{n}_i(\bar{t}_j)\right)\right)$.
  7: $\bar{\sigma}_{\max}(k+1) = (1/J)\sum_{j=1}^{J} I \left(\bar{d}_j - \bar{t}_j > T_{\max}\left(i, \bar{n}_i(\bar{t}_j)\right)\right)$.
  8:
$$
\begin{aligned}
n_i^{\Delta}&(k+1) \\
&= I\left(\bar{\sigma}_{\min}(k+1) > \epsilon_1\right) - I\left(\bar{\sigma}_{\max}(k+1) > \epsilon_2\right) \\
&\quad + I(\hat{n}_i(k+1) + I\left(\bar{\sigma}_{\min}(k+1) > \epsilon_1\right) \\
&\quad - I(\bar{\sigma}_{\max}(k+1) > \epsilon_2) < 0).
\end{aligned}
$$
  9: $\bar{n}_i(k+1) = \hat{n}_i(k+1) + n_i^{\Delta}(k+1)$.
10: **end for**
11: $k = k + 1$.
12: **if** $k \leq T$ **then**
  13: Go to step 2.
14: **else**
  15: Stop.
16: **end if**

Algorithm 3 Naive estimation with correction and propagation

1: Initialize $\bar{n}_i(0), i = 1, \ldots, N, k = 0$. Set ϵ_1 and ϵ_2.
2: Observe $\hat{e}_{i,j}(k), (i,j) \in \mathcal{E}$. Set $n_i^{\Delta}(k+1) = 0, i \in \mathcal{V}$.
3: **for** $i = 1$ to N **do**
  4: $\hat{n}_i(k+1) = \bar{n}_i(k) - \hat{e}_{i,*}(k) + \hat{e}_{*,i}(k)$.
  5: Update the series of (occupant level, departure time) pair $\left(\bar{n}_i(\bar{t}_j), \bar{d}_j - \bar{t}_j\right), j = 1, \ldots, J$.
  6: $\bar{\sigma}_{\min}(k+1) = (1/J)\sum_{j=1}^{J} I \left(\bar{d}_j - \bar{t}_j \leq T_{\min}\left(i, \bar{n}_i(\bar{t}_j)\right)\right)$.
  7: $\bar{\sigma}_{\max}(k+1) = (1/J)\sum_{j=1}^{J} I \left(\bar{d}_j - \bar{t}_j > T_{\max}\left(i, \bar{n}_i(\bar{t}_j)\right)\right)$.
  8:
$$
\begin{aligned}
n_i^{\Delta}&(k+1) \\
&= I\left(\bar{\sigma}_{\min}(k+1) > \epsilon_1\right) - I\left(\bar{\sigma}_{\max}(k+1) > \epsilon_2\right) \\
&\quad + I(\hat{n}_i(k+1) + I\left(\bar{\sigma}_{\min}(k+1) > \epsilon_1\right) \\
&\quad - I(\bar{\sigma}_{\max}(k+1) > \epsilon_2) < 0) + n_i^{\Delta}(k+1).
\end{aligned}
$$
  9: **if** $n_i^{\Delta}(k+1) = 1$ **then**
    10: Pick $j \in A_i$ w.p. $p_{j,i}^{+1}$.
    11: $n_j^{\Delta}(k+1) = n_j^{\Delta}(k+1) - 1$.
  12: **else if** $n_i^{\Delta}(k+1) = -1$ **then**
    13: Pick $j \in A_i$ w.p. $p_{i,j}^{-1}$.
    14: $n_j^{\Delta}(k+1) = n_j^{\Delta}(k+1) + 1$.
  15: **end if**
16: **end for**
17: $\bar{\mathbf{n}}(k+1) = \hat{\mathbf{n}}(k+1) + \mathbf{n}^{\Delta}(k+1)$.
18: $k = k + 1$.
19: **if** $k \leq T$ **then**
  20: Go to step 2.
21: **else**
  22: Stop.
23: **end if**

V. Numerical Results

Here, we demonstrate the performance of the algorithms by simulation results in Section V-A and by field test in Section V-B.

A. Simulation Results

1) Layout 1: The layout in Fig. 2(a) is part of the FIT building in Tsinghua University, Beijing, China, where zones 1–11 are rooms, zones 12 and 13 are corridors, and zones 14 and 15 are exits. Instead of assuming a Markovian movement model for the occupants, we have used video cameras to tape the movement

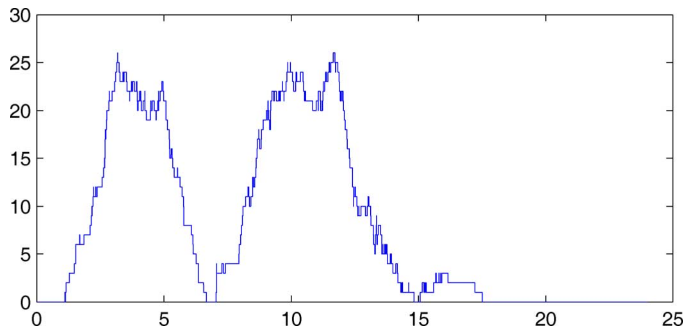

Fig. 5. Total number of occupants in the rooms and corridors throughout a day. (x-axis: hour; y-axis: occupant level).

of the occupants and manually obtained the ground truth for a single day. The total number of occupants in the room zones and corridor zones are shown in Fig. 5. We use these real trajectories of the occupants in our simulation. The randomness comes from the sensors and the estimation methods.

To apply algorithms 2 and 3, we set $\epsilon_1 = 0.001$, $\epsilon_2 = 0.001$. We discretize the time and let each stage be 1 s. In order to calculate $T_{\min}$ and $T_{\max}$, we need to estimate $p_{i,i}$, which is the probability for an occupant to stay in the same zone after one stage. This probability depends on the zone. We divide the zones into two groups, namely the room zones and corridor zones. For the room zones, suppose that the occupant may stay in the zone for longer than $T_1 = 4$ hours w.p. ϵ_2. Then, we have

$$p_{i,i}^{T_1} = \epsilon_2, \quad i = 1, \ldots, 11.$$

Therefore, $p_{i,i} = 0.9995, \ \ i = 1, \ldots, 11$. For corridor zones, suppose that the occupant may stay in the zone for longer than $T_2 = \ 10$ s w.p. ϵ_2. Then, we have

$$p_{i,i}^{T_2} = \epsilon_2, \qquad i = 12, 13. \tag{7}$$

Therefore, $p_{i,i} = 0.5012, \ \ i = 12, 13$. Note that this probability is only used in the algorithms to generate the estimation, but not to simulate the movement of the occupants. As aforementioned, the movement of the occupants in the simulation are from the ground truth and are fixed.

Infrared beam sensors are deployed on each edge, which usually do not have false alarms. These sensors do have miss detection w.p. $p_s^0 = 0.005$, and even mistakenly detect the moving direction of the occupants w.p. $p_s^{-1} = 0.005$. Overall speaking, if an occupant passes such an infrared beam sensor, this event is detected correctly w.p. $p_s^1 = 0.99$.

We are interested in the error rate of the following four methods.

NE	Implement algorithm 1 in all of the zones.
M1	Implement algorithm 2 only in the corridor zones.
M2	Implement algorithm 2 in all of the zones.
M3	Implement algorithm 3 in all of the zones.

Assume that the initial distribution of the occupants are known to the methods, i.e., $\bar{n}_i(0) = 0, \ \ i \neq 14$. Then, the error rate curves for the four methods are shown in Fig. 6(a). We can see that M1 has smaller mean error rate than NE, which

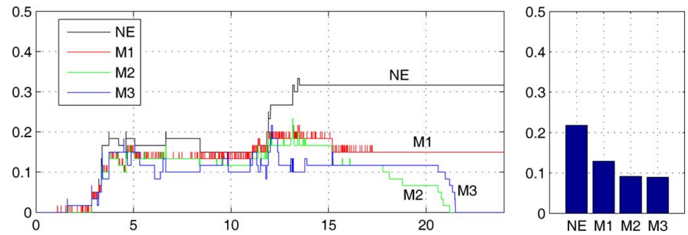

Fig. 6. Error rate curves of the four methods with perfect knowledge on the initial occupant distribution. (x-axis: hour; y-axis: error rate).

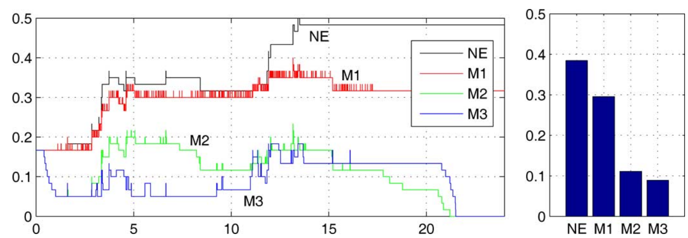

Fig. 7. Error rate curves of the four methods with imperfect knowledge on the initial occupant distribution. (x-axis: hour; y-axis: error rate).

shows that rule 1 helps to reduce the error. M2 is better than M1 because rule 1 is applied to all of the zones in M2 but only to the corridor zones in M1. M3 is the best, because both rules are applied. We can also see that NE has accumulative error over the time, i.e., if an error happens early in the morning, that error will remain in the estimation until the system is reset. Though M1 can cancel part of these accumulative error, such a cancellation only applies to the corridors and are not propagated. Therefore, M1 also has accumulative error. M2 and M3 manage to cancel the accumulative error by the end of the day. This is a nice feature comparing with NE.

2) Impact of Knowledge on the Initial Distribution: Assume that the knowledge of the initial distribution of the occupants are subject to error. We show the error rate curves for the four methods in Fig. 7(a) and the mean error rate in Fig. 7(b). We can see that the initial error significantly degrades the performance of NE and M1. M2 and M3 successfully reduce the error rate in the beginning. The mean error rate of M2 is slightly higher than that in Fig. 6(b). The performance of M3 almost is not affected by the initial error. This shows that M3 is robust to the initial error. Note that traditional methods such as NE usually require to start from the midnight when the building is usually empty, so the performance degradation that is caused by imperfect initial knowledge can be minimized. However, the above results show that M3 can start from any time in a day, which is much more flexible.

3) Impact of Occupant Population: Recall that Z is the total number of occupants in the building. From Fig. 5, we can see that $Z < 30$ in the previous simulations. In order to demonstrate the performance of the four methods under different occupant population, let $Z = 10, 20, \ldots, 100$. We assume that the movement of the occupants follow a Markov chain. Using the ground truth of the trajectories, we estimate the transition probabilities $p_{i,j}$. For each value of Z, we use five replications to estimate the average mean error rate of the four methods and show in Fig. 8. We can see that M1, M2, and M3 are better than NE. M2 and

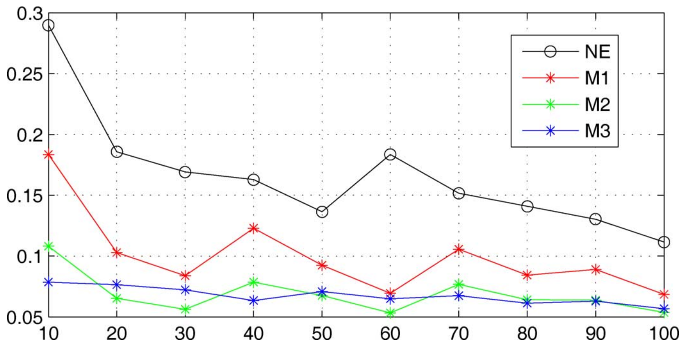

Fig. 8. Mean error rate of the four methods under different occupant populations (averaged over five replications).

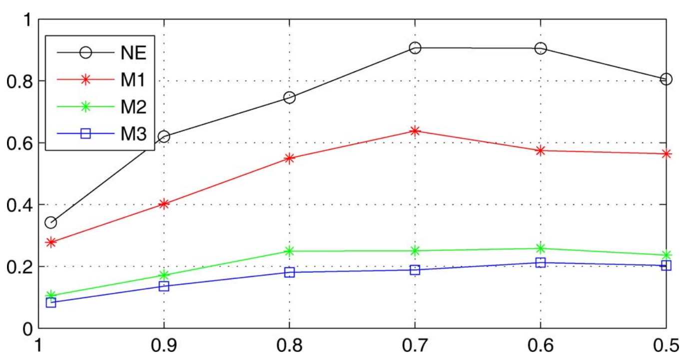

Fig. 9. Mean error rate of the four methods under different sensing accuracies (averaged over five replications).

M3 are better than M1. The average mean error rate of all of the four methods reduce when the occupant population increases. One reason is that when there are more occupants in the area, miscounts and overcounts tend to cancel each other more often. This leads to a smaller error rate.

4) Impact of Sensing Accuracies: Consider different sensing accuracies. Let the probability of correct sensing $p_s^1 = 0.5$, 0.6, 0.7, 0.8, 0.9, and 0.99. For each value of p_s^1, let $p_s^0 = p_s^{-1} = (1 - p_s^1)/2$, respectively. Let $Z = 30$. We run five replications and show the average mean error rate of the four methods in Fig. 9. We can see that the performance of all four methods become worse when the sensors are less accurate. M3 performs better than M2, which in turn is better than M1. NE performs the worst. It is noticed that the mean error rate of the NE method starts to drop when the sensing accuracies p_s^1 drops beyond 0.7. One reason is that in our sensor model, when p_s^1 is low, both miss detection and detection with reverse direction occur more often. This makes the observed occupant level in some zones reach negative more often. Because in the NE method, the observed occupant level will be corrected to 0 if it is negative, this correction helps to reduce the error rate. In short, M3 performs the best under all of the sensing accuracies.

5) Impact of Topology: In order to test the impact of the topology, we consider another layout as shown in Fig. 10. There are eight zones in total. Zones 1–3 are rooms. Zones 4–6 are corridors. Zones 7 and 8 are exits. Note that the graph model of layout 1 (Fig. 2) is a tree, but there are cycles in Fig. 10. There are 30 occupants in total. All of the occupants are in node 7 in the beginning. Their movements follow a Markov chain.

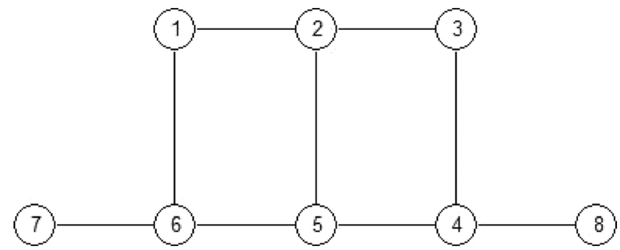

Fig. 10. Layout 2.

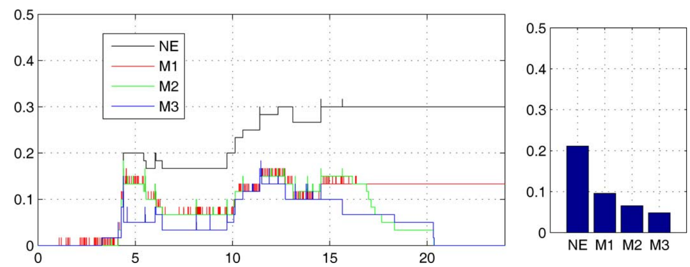

Fig. 11. Error rate curves of the four methods with perfect knowledge on the initial occupant distribution. (x-axis: hour; y-axis: error rate).

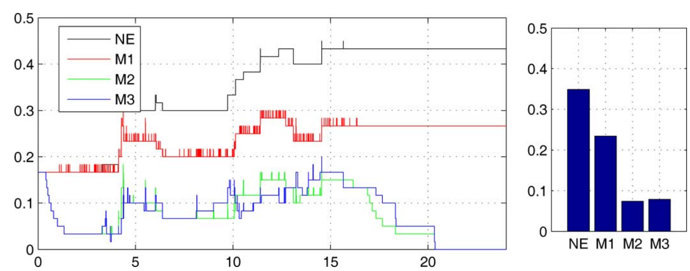

Fig. 12. The error rate curves of the four methods with imperfect knowledge on the initial occupant distribution. (x-axis: hour; y-axis: error rate).

We follow the parameter setting in Section V-A1 and set $p_{i,i} = 0.9995$ for $i = 1, 2, 3$ and $p_{i,i} = 0.5012$ for $i = 4, 5, 6$. We assume that the occupants move among the neighboring zones with equal probabilities, i.e., $p_{i,j} = 1/|A_i|, i \neq j$. The sensor model is $p_s^1 = 0.99$, $p_s^0 = 0.005$, $p_s^{-1} = 0.005$. When the initial distribution of the occupants are known, the error rate curves for the four methods are shown in Fig. 11. When the knowledge of the initial distribution is subject to error, the error rate of the four methods are shown in Fig. 12. We can see that M3 is better than M2, M2 is better than M1, and M1 is better than NE in both cases. NE and M1 have positive terminal error rate. M2 and M3 successfully remove all the accumulative error by the end of the day.

B. Field Test

We use layout 1 to run the field test. Recall that this is part of an office building in the campus. Infrared beam sensors are deployed on each edge to monitor the edge-crossing events. Video cameras are used to record the movement of the occupants. We then obtain the ground truth manually. In order to make the estimation system easily scale up, we test a decentralized version of the methods. In particular, a computing node is deployed in each zone. When a sensor detects an event, this information is sent to the computing nodes in both zones. All four methods

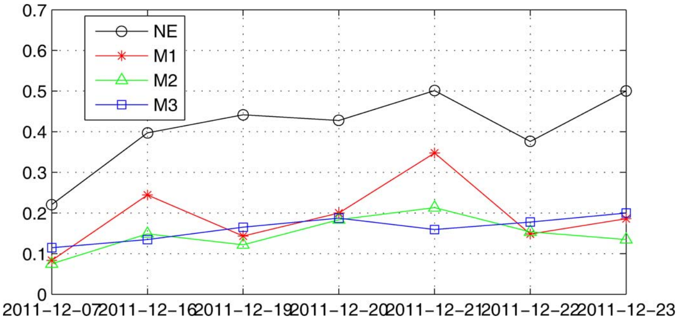

Fig. 13. Mean error rate of the four the methods in the field test of seven days. (x-axis: date; y-axis: mean error rate).

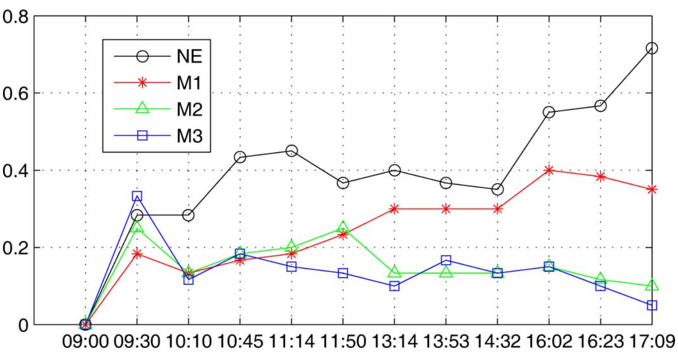

Fig. 14. Error rate curves of the four methods in one day in the field test. (x-axis: time; y-axis: error rate).

are implemented in the same time, and decentralized in each computing node. The estimations are transmitted to a computer simply for record. By comparing the estimated occupant distribution with the ground truth, the error rate can be calculated. The daily mean error rates of the four methods in seven days are shown in Fig. 13. We also show the error rate curve in a particular day in Fig. 14. We can see that M1, M2, and M3 are better than NE. NE has a significantly large terminal error rate. By applying rule 1 to the corridors, M1 achieves a small terminal error rate. By further applying rule 1 to all of the zones and incorporating rule 2, M2 and M3 achieve much smaller terminal error rates, respectively. Note that the performance of M2 and M3 is much better than NE and M1 in the afternoon in Fig. 14. This is because that there are many arrival and departure events in that afternoon, which improves the estimation of $\bar{\sigma}_{\min}$ and $\bar{\sigma}_{\max}$ and improves the performance of M2 and M3.

VI. Conclusion

In this paper, we consider zonal occupant distribution estimation in buildings. Two rules are developed. Rule 1 compares the stay time and the estimated occupant level. Under the assumption that more occupants in a zone lead to faster departure, a correction term to the estimation may be generated. Rule 2 then propagates this correction to the neighboring zones to keep the total number of occupants as a constant. The performance of the two rules are demonstrated by simulations and field tests. The results show that both rules reduce the error rate. When combined together, these rules usually can cancel the accumulative error by the end of the day. These rules have good performance under imperfect knowledge of the initial occupant distribution, different occupant population, different sensing accuracies, and different layouts. Also, these rules can be implemented in a decentralized way as shown in the field test.

Note that when multiple sensing systems exist on the edge, fusing these information usually improve the sensing accuracy, which can improve the performance of the two rules. Also, if there are sensors in each zone to detect whether the zone is occupied or not, this information can be used to further improve the two rules.

References

[1] N. Djuric, V. Novakovic, J. N. Holst, and Z. Mitrovic, “Optimization of energy consumption in buildings with hydronic heating systems considering thermal comfort by use of computer-based tools,” *Energy and Buildings*, vol. 39, no. 4, pp. 471–477, 2007.

[2] R. Yang and L. F. Wang, “Energy management of multi-zone buildings based on multi-agent control and particle swarm optimization,” in *Proc. IEEE Int. Conf. Syst., Man, Cybernet.*, Anchorage, AL, USA, 2011, pp. 159–164.

[3] G. Tan and L. R. Glicksman, “Application of integrating multi-zone model with cfd simulation to natural ventilation prediction,” *Energy and Buildings*, vol. 37, no. 10, pp. 1049–1057, 2005.

[4] V. L. Erickson and A. E. Cerpa, “Occupancy based demand response HVAC control strategy,” in *Proc. 2nd ACM Workshop on Embedded Sensing Syst. for Energy-Efficiency in Buildings*, Zurich, Switzerland, 2010, pp. 7–12.

[5] J. Zhang, R. G. Lutes, G. Liu, and M. R. Brambley, “Energy Savings for Occupancy-Based Control (OBC) of Variable-Air-Volume (VAV) Systems,” Pacific Northwest Nat. Lab., Richland, WA, USA.

[6] T. Chen, L. Pan, H. Zhang, S. Narayanan, and N. Soldner, “Experimental study of evacuation from a 4-story building,” in *Proc. Ninth Asia–Oceania Symp. Fire Science and Technol.*, 2013, vol. 62, pp. 538–547.

[7] P. Bahl and V. N. Padmanabham, “Radar: An in-building RF-based user location and tracking system,” in *Proc. IEEE INFOCOM*, 2000, pp. 775–784.

[8] J. Hightower, R. Want, and G. Borriello, “Spoton: An indoor 3D location sensing technology based on RF signal strength,” Dept. Comput. Sci. Eng. Univ. Washington, Seattle, WA, USA, 2000, Tech. Rep. UW CSE 00-02-02.

[9] L. M. Ni, Y. Liu, Y. C. Lau, and A. P. Patil, “Landmarc: Indoor location sensing using active RFID,” *Wireless Networks*, vol. 10, pp. 701–710, 2004.

[10] Ekahau Positioning Engine 2.0 Ekahau, Inc. [Online]. Available: http://www.ekahau.com

[11] P. Steggles and S. Gschwind, “The Ubisense Smart Space Platform,” Tech. Rep. Ubisense Limited, 2005.

[12] Z. N. Zhen, Q. S. Jia, C. Song, and X. H. Guan, “An indoor localization algorithm for lighting control using rfid,” in *Proc. IEEE Energy 2030 Conf.*, Atlanta, GA, USA, Nov. 17–18, 2008, pp. 1–6.

[13] R. Want, A. Hopper, and V. Falcao, “The active badge location system,” *ACM Trans. Inf. Syst.*, vol. 10, no. 1, pp. 91–102, 1992.

[14] N. B. Priyantha, A. Chakraborty, and H. Balakrishnan, “The Cricket location-support system,” in *Proc. 6th Annu. Int. Conf. Mobile Comput. Netw..*, Boston, MA, USA, 2000, pp. 32–43.

[15] H. T. Wang, Q. S. Jia, C. Song, R. Yuan, and X. H. Guan, “Estimation of occupancy level in indoor environment based on heterogeneous information fusion,” in *Proc. 49th IEEE Conf. Decision and Control*, Atlanta, GA, USA, Dec. 15–17, 2010, pp. 5086–5091.

[16] J. W. Li, L. Huang, and C. P. Liu, “Robust people counting in video surveillance: Dataset and system,” in *Proc. Eighth IEEE Int. Conf. Adv. Video Signal-Based Surveillance*, 2011, pp. 54–59.

[17] C. H. Chen, Y. C. Chang, T. Y. Chen, and D. J. Wang, “People counting system for getting in/out of a bus based on video processing,” in *Proc. of the 8th Internat. Conf. on Intelligent Syst. Design and Applicat.*, 2008, pp. 565–569.

[18] C. Pornpanomchai, T. Liamsanguan, and V. Vannakosit, “Vehicle detection and counting from a video frame,” in *Proc. Int. Conf. Wavelet Analys. Pattern Recognit.*, 2008, pp. 356–361.

[19] S. Meyn, A. Surana, Y. Lin, S. M. Oggianu, S. Narayanan, and T. A. Frewen, “A sensor-utility-network method for estimation of occupancy distribution in buildings,” in *Proc. 48th IEEE Conf. Decision and Control*, Shanghai, China, Dec. 16–18, 2009, pp. 1494–1500.

[20] J. Hutchins, A. Ihler, and P. Smyth, "Modeling count data from multiple sensors: A building occupancy model," in *Proc. IEEE Int. Workshop Computat. Advances in MultiSensor Adaptive Process.*, 2007.

[21] J. Hutchins, "Modeling count data from multiple sensors: A building occupancy model," in *Proc. 2nd IEEE Int. Workshop on Computat. Advances in Multi-Sensor Adaptive Process.*, 2007, pp. 241–244.

[22] J. Page, D. Robinson, N. Morel, and J. L. Scartezzini, "A generalised stochastic model for the simulation of occupant presence," *Energy and Buildings*, vol. 40, pp. 83–98, 2008.

[23] F. Tang and A. Ren, "Agent-based evacuation model incorporating fire scene and building geometry," *Tsinghua Sci. Technol.*, vol. 13, no. 5, pp. 708–714, 2008.

[24] S. M. V. Gwynne and E. D. Kuligowski, "Simulating a building as a people movement system," *J. Fire Sciences*, vol. 27, pp. 343–368, 2009.

[25] C. Liao and P. Barooah, "A novel stochastic agent-based model of building occupancy," in *Proc. Amer. Control Conf.*, San Francisco, CA, USA, 2011, pp. 2095–2100.

Qing-Shan Jia (S'02–M'06–SM'11) received the B.E. degree in automation and Ph.D. degree in control science and engineering from Tsinghua University, Beijing, China, in 2002 and 2006, respectively.

He is currently an Associate Professor with the Center for Intelligent and Networked Systems (CFINS), Department of Automation, TNLIST, Tsinghua University, Beijing, China. He was a Visiting Scholar with Harvard University, in 2006, with the Hong Kong University of Science and Technology in 2010, and with Massachusetts Institute of Technology in 2013. His research interests include theories and applications of discrete event dynamic systems and simulation-based performance evaluation and optimization of complex systems.

Hengtao Wang (M'12) received the B.E. degree in automation from Xi'an Jiaotong University, China, in 2007. He is currently working toward the Ph.D. degree at the Center for Intelligent and Networked Systems (CFINS), Department of Automation, Tsinghua University, Beijing.

His research interests include wireless sensor network, information fusion, reconfigurable networked system and occupant localization and counting in building.

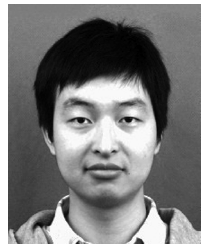

Yulin Lei (M'14) received the B.E. degree in automation from University of Science and Technology of China, Hefei, China, in 2011. He is currently working toward the master degree at the Center for Intelligent and Networked Systems (CFINS), Department of Automation, Tsinghua University, Beijing.

His research interests include energy consumption monitoring and occupant monitoring in building.

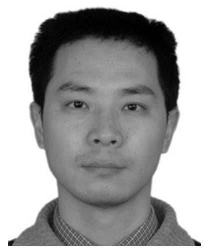

Qianchuan Zhao (M'06–SM'08) received the B.E. degree in automatic control, B.S. degree in applied mathematics, and Ph.D. degree in control theory and its applications from Tsinghua University, Beijing, China, in 1992, 1992, and 1996, respectively.

He is currently a Professor and Associate Director of the Center for Intelligent and Networked Systems (CFINS), Department of Automation, Tsinghua University, Beijing, China. He was a Visiting Scholar with Carnegie-Mellon University and Harvard University in 2000 and 2002, respectively. He was a Visiting Professor with Cornell University in 2006. His research interests include discrete event dynamic systems theory and applications, optimization of complex systems, and wireless sensor networks.

Xiaohong Guan (M'93–SM'95–F'07) received the B.S. and M.S. degrees in control engineering from Tsinghua University, Beijing, China, in 1982 and 1985, respectively, and the Ph.D. degree in electrical engineering from the University of Connecticut, Storrs, CT, USA, in 1993.

He was a Senior Consulting Engineer with PG&E from 1993 to 1995. He visited the Division of Engineering and Applied Science, Harvard University, from January 1999 to February 2000. Since 1995 he has been with the Systems Engineering Institute, Xian Jiaotong University, Xi'an, China, and appointed as the Cheung Kong Professor of Systems Engineering since 1999, and as the Dean of School of Electronic and Information Engineering since 2008. Since 2001 he has also been the Director of the Center for Intelligent and Networked Systems, Tsinghua University, Beijing, China, and served as the Head of the Department of Automation from 2003 to 2008. His research interests include complex networked systems including smart power grid, planning and scheduling of electrical power and manufacturing systems, and electric power markets.